DOI: 10.1002/eej.23117

RESEARCH ARTICLE

WILEY

Design of a coil geometry for generating magnetic field to evaluate biological effects at 85 kHz

Kazuki Matsubara | Keiji Wada | Yukihisa Suzuki

Tokyo Metropolitan University, Tokyo, Japan

Correspondence
Yukihisa Suzuki, Tokyo Metropolitan University, Tokyo, Japan.
Email: y_suzuki@tmu.ac.jp

Abstract

In recent years, the use of induction-heating systems has increased and wireless power transmission (WPT) systems have been discussed. These applications are installed close to a human body. Therefore, it is important to discuss the effects of alternating magnetic fields and to evaluate electromagnetic interference. This paper discusses the design procedure of a magnetic field generator to evaluate the electromagnetic interference at 85 kHz that is being studied in WPT systems for EV and HEV. The magnetic field generator presented in this paper consists of a single-phase inverter circuit that uses SiC-MOSFETs and an air–core inductor that is used as the coil for generating a magnetic field. In particular, this paper shows that the coil used for generating magnetic field needs to reduce the winding voltage to generate higher magnetic flux. In addition, this paper presents the design procedure of the proposed coil structure that can satisfy some limited conditions. The experimental results of the proposed system rated at 82 kHz and 100 A are presented.

KEYWORDS

breakdown voltage, coil structure, magnetic field generator, magnetic flux density

1 | INTRODUCTION

In the recent years, induction heating devices using magnetic field of 20 kHz to 100 kHz have spread rapidly in both industrial[1] and home[2,3] applications. In addition, 85-kHz wireless power transmission (WPT) systems were proposed for electric vehicles, and extensive research and development (R&D) is conducted on power supplies, power transmission coils, and other components.[4–7] Transmission coils of WPT systems for electric vehicles are supposed to be used in the vicinity of other electronic devices and human bodies, and there are concerns about electromagnetic interference and biological effects due to alternating magnetic fields generated by these coils. Therefore, biological effects of 85-kHz alternating magnetic fields must be evaluated through experiments.[8–10]

Some systems were developed to evaluate biological effects of alternating magnetic fields; there are reports about systems operated at 200 Hz to 100 kHz.[11–14] We studied experimental systems to evaluate biological effects of 85-kHz magnetic field, and explored structure of magnetic field generators using air–core solenoid coils.[15] However, with double-layer solenoid coils offering optimal magnetic flux density, voltage of the kilovolt order may occur between coil windings, and possibility of dielectric breakdown must be taken into account in design of magnetic field generation coils.

In this paper, we aim at development of a magnetic field generator in 85-kHz band intended for evaluation of biological effects; particularly, we propose a double-layer solenoid coil with reduced maximum voltage between windings. First, in order to combine winding voltage reduction with magnetic flux density output comparable to conventional design, we propose an improved structure of double-layer solenoid coil, and demonstrate usefulness of this coil in magnetic field generation for evaluation of biological effects. Then, we derive a practical coil structure by numerical analysis, and manufacture a prototype of double-layer solenoid coil with water-cooling copper pipes. In addition, we show through experiments that winding voltage can be reduced in the prototype coil. Finally, we conduct experiments at 82 kHz and 100 A

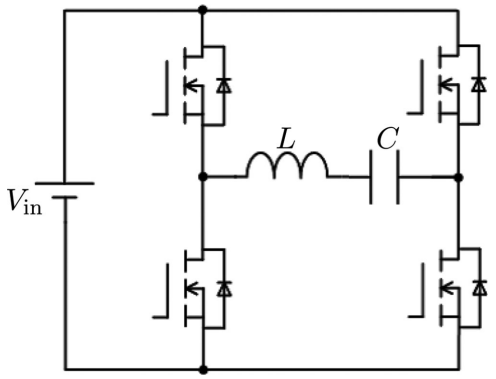

FIGURE 1 Full-bridge inverter and *LC* series resonant circuit

with a circuit in which a resonant capacitor and the improved solenoid coil are connected in series to single-phase output using MOSFET to confirm that the proposed coil can be used for evaluation of biological effects.

2 | CIRCUIT CONFIGURATION OF MAGNETIC FIELD GENERATOR

2.1 | Design issues

Magnetic field generator for evaluation of biological effects produces magnetic field when sine current flows in air–core coil. In this study, as shown in Figure 1, an *LC* series resonant circuit is connected to ac side of a voltage-fed inverter (power source) with square wave output to produce sine current in the coil. Here, resonant inductor is a coil for magnetic field generation. Air–core solenoid coil with inner diameter of 10 cm or larger is assumed as the magnetic field generation coil so that a biological object exposed to magnetic field can be placed inside the coil. Figure 2 illustrates design issues of coil used for magnetic field generation in this study. Under the above assumptions, design of magnetic field generation coil involves following three items to be considered.

1. Magnetic flux density in the middle part of solenoid coil
2. Coil terminal voltage, resonant capacitor-rated voltage

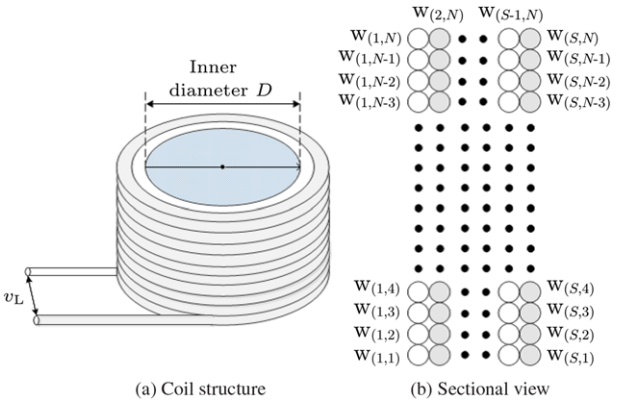

FIGURE 3 Coil structure and sectional view of solenoid coil [Color figure can be viewed at wileyonlinelibrary.com]

3. Coil temperature during continuous operation

Target value of magnetic flux density can be defined so that electric field induced inside a biological object inserted in the coil exceeds the guidelines of International Commission on Non-Ionizing Radiation Protection (ICNIRP) (see the Appendix). Thus, in this study, magnetic flux density in the middle part is set to 20 mT or higher.

Since *LC* series resonant circuit is adopted in this study, there is a risk that coil terminal voltage and resonant capacitor voltage reach the kV order. Therefore, coil terminal voltage and resonant capacitor-rated voltage must be taken into account in design. In addition, continuous operation of magnetic field generator for 1 h or longer is required for evaluation of biological effects. Under this condition, temperature inside the coil during experiments must be kept at room temperature of 25 ± 3°C so that only magnetic field effects on biological objects can be evaluated. Below, we consider an air-core solenoid coil with inner diameter of 11 cm provided with water-cooling copper pipes.

2.2 | Solenoid coil structure

Structure of the solenoid coil for magnetic field generator is shown in Figure 3. In the diagram, N is the number of turns per

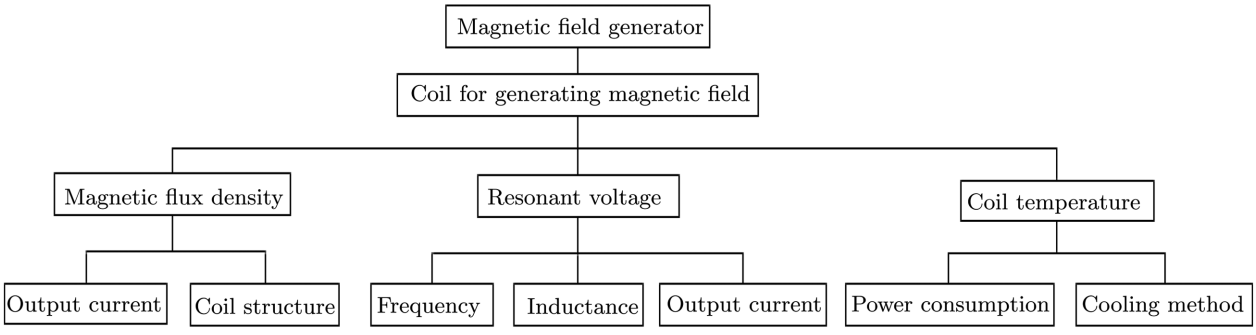

FIGURE 2 Classification of coil design for generating magnetic field

layer, S is the number of layers, and $w_{(\text{Layer number, Turn number})}$ is the corresponding one-turn winding portion. In a multilayer winding coil, windings are wound in the order of $w_{(1,1)}$ to $w_{(1,N)}$, $w_{(2,N)}$ to $w_{(2,1)}$, and then again $w_{(3,1)}$, $w_{(3,N)}$. In so doing, peak value V_L of coil terminal voltage is expressed as follows:

$$V_{\mathrm{L}} = 2\pi f_{\mathrm{s}} L I_{\mathrm{p}}. \tag{1}$$

Here, f_s is the switching frequency, L is the inductance, and I_{p} is the current amplitude. Maximum value of coil terminal voltage is determined by both dielectric strength between input/output terminals and withstand voltage of resonant capacitor. In this study, maximum value of coil terminal voltage is set to $V_{\mathrm{L}} = 10\ \mathrm{kV_{peak\text{-}peak}}$. From Equation (1), the upper limit of inductance is 66.2 μH at switching frequency of 85 kHz and current effective value of 100 A ($I_{\mathrm{p}} = 141$ A).

2.3 | Analysis of coil parameters

With reference to the design values mentioned above, we analyze coil structure, inductance, and flux density at coil center, thus aiming at optimal coil structure for practical generation of magnetic field.[16] Inductance of magnetic field generation coil consists of internal inductance L_{in}, external inductance L_{e}, and interwinding mutual inductance M. Equation (2) gives internal inductance L_{in}; here, l denotes the wiring length and μ_0 is the permeability of vacuum:

$$L_{\mathrm{in}} = \frac{\mu_0 l}{8\pi}. \tag{2}$$

Similarly, Equation (3) gives external inductance L_{e} of one-turn coil; here D is the distance to coil center and r is the conductor radius:

$$L_{\mathrm{e}} = \mu_0 R\left(\log\frac{8(D+r)}{r} - 2\right). \tag{3}$$

Similarly, Equation (4) gives mutual inductance M in case two circular coils with radiuses a and b are arranged on the same vertical axis at distance d:

$$M = \mu_0\sqrt{ab}\left(\left(\frac{2}{k} - k\right)K(k) - \frac{2}{k}E(k)\right), \tag{4}$$

$$k^2 = \frac{4ab}{(a+b)^2 + d^2}.$$

In Equation (4), $K(k)$ and $E(k)$ are complete elliptic integrals of the first and second kinds, respectively. Coil's total inductance can be calculated using Equations (2) to (4) for every winding as shown in Equation (5).

$$L_{\mathrm{Coil}} = \sum_{n=1}^{N}\sum_{s=1}^{S}\left(L_{\mathrm{in}} + L_{\mathrm{e}} + \sum_{n=1}^{N}\sum_{s=1}^{S} M\right). \tag{5}$$

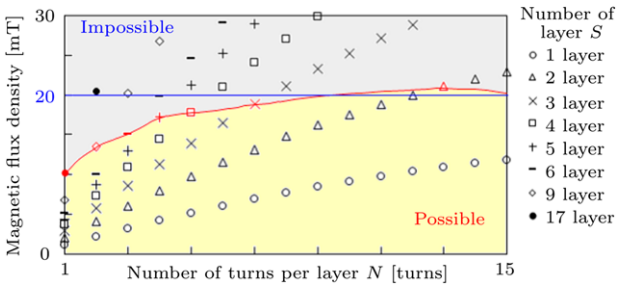

FIGURE 4 Calculation results for inductance and magnetic flux density [Color figure can be viewed at wileyonlinelibrary.com]

Magnetic flux density on coil's central axis can be found using Bio-Savart law. In our analysis, coil center is placed at the origin of z-axis. Equation (6) gives z-axis component of magnetic flux density at a distance h from coil placed on z-axis when current I flows in the coil:

$$B_z(h) = \sum_{n=1}^{N}\sum_{s=1}^{S}\frac{\mu_0 R^2(s) I}{2\{R^2(s) + Z^2(h,n)\}^{3/2}}, \tag{6}$$

$$R(s) = \frac{D}{2} + r(2s-1),$$

$$Z(h,n) = h + r(N - 2n + 1).$$

Here, $R(s)$ is the distance from coil center to winding center, being a function of the layer number s. Similarly, $Z(h,n)$ is the distance between every winding and flux density calculation point; this distance can be expressed as a function of distance h between coil center and calculation point, and turn number n.

2.4 | Solenoid coil design

We calculate inductance and magnetic flux density for the coil structure in Figure 3; the number N of turns per layer and number of layers S are treated as parameters. Figure 4 shows calculated flux density in case that effective value of coil current is 100 A; here, the horizontal axis plots number of turns per layer, and the vertical axis plots flux density at coil center. In the diagram, the red line shows the boundary of upper limit of inductance (66.2 μH) for each number of turns. This means that coil terminal voltage lies within its upper limit in the region where number of turns and number of layers are below the boundary. As indicated by the diagram, an allowed inductance of 61.6 μH can be designed with a structure of 2 layers and 13 turns. In so doing, magnetic flux density at coil center is 21.1 mT.

Thus, flux density of 20 mT can be outputted at coil terminal voltage below $10\ \mathrm{kV_{peak\text{-}peak}}$. However, in case of double-layer solenoid coil, terminal voltage applies between the windings $w_{(1,1)}$ and $w_{(2,1)}$, and insulation breakdown between

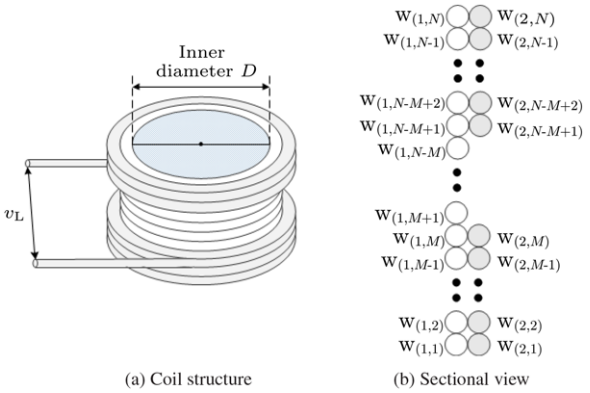

FIGURE 5 Proposed coil structure with N turns in inner layer and M turns in outer layer [Color figure can be viewed at wileyonlinelibrary.com]

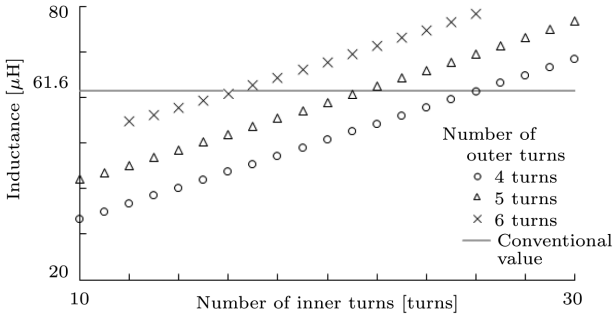

FIGURE 6 Calculation results for inductance

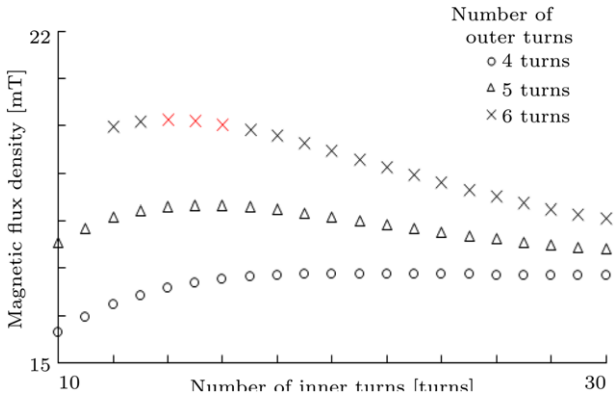

FIGURE 7 Calculation results for magnetic flux density at center point of coil [Color figure can be viewed at wileyonlinelibrary.com]

windings inside the coil is a problem even though the terminal voltage is kept below 10 $kV_{peak\text{-}peak}$.

3 | COIL STRUCTURE WITH REGARD TO WINDING VOLTAGE

3.1 | Improved solenoid coil

Here, we consider a coil structure to reduce interwinding voltage as compared to the exiting solenoid coil.

Improved solenoid coil structure proposed in this study is shown in Figure 5A. Besides, cross section of the improved solenoid coil is shown in Figure 5B. As explained above section, double-layer structure is optimal for the solenoid coil; thus, we consider the improved coil with two layers. With the first and second layers defined as inner and outer layers, respectively, windings of the outer layer in the improved coil are divided into upper and lower sections as shown in Figure 5(B), while no windings exist in the middle part. In this study, the number of turns in upper and lower sections is same so that a symmetrical distribution of magnetic flux is obtained inside the coil. Below, the improved solenoid coil with N turns in the inner layer and M turns in upper and lower sections of the outer layer is referred to as N-M turns coil. Besides, same as with conventional solenoid coil, one-turn winding portion is denoted by $w_{(\text{Layer, Turn})}$. In Figure 5B, coil current flows from $w_{(2,N\text{-}M+1)}$ via $w_{(2,N)}$, $w_{(1,N)}$, $w_{(1,1)}$, $w_{(2,1)}$ to $w_{(2,M)}$.

3.2 | Inductance analysis

Figure 6 results of inductance analysis at varied number of turns in the inner and outer layers, the inner diameter, and conductor diameter being, respectively, 11 cm and 3.59 mm. The horizontal axis plots number of turns in the inner layer, and the vertical axis plots inductance. In the diagram, the black line pertains to the inductance of conventional solenoid coil (61.6 μH). As can be seen from the plot, inductance of the improved coil is affected by number of outer turns stronger than by number of inner turns.

3.3 | Magnetic flux density analysis

Figure 7 shows results of magnetic flux density analysis at the center of the coils with different parameters. Here, coil current was set to 100 A. In the diagram, the horizontal axis plots number of turns in the inner layer, and the vertical axis plots magnetic flux density at the coil center. In a typical coil, magnetic flux density inside the coil grows with more turns. However, with the improved solenoid structure, outer layer windings move away from the center when number of turns in the inner layer is increased; thus, if number of turns is increased only in the inner layer, then the influence of the outer layer windings decreases, and magnetic flux density at the center declines. As a result, relationship between number of turns and magnetic flux density becomes as shown in Figure 7. On the other hand, as can be seen from Figure 7, using more turns in the outer layer is efficient to increase magnetic flux density at the coil center. Besides, six outer turns are needed for the coil to generate 20 mT, and constraints on both inductance and flux density are met by five structures, namely, 12 to 6 through 16 to 6 turns.

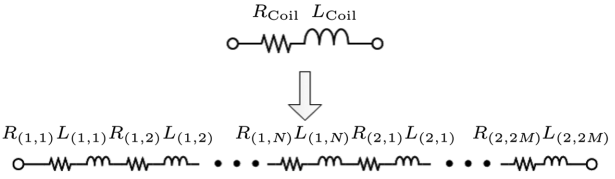

FIGURE 8 Equivalent circuit dividing each winging of coil

3.4 | Winding voltage analysis

Based on the results of Figure 7, below we analyze maximum interwinding voltage for coils with three structures, namely, 14 to 6, 15 to 6, and 16 to 6 turns coils. Particularly, we evaluate maximum winding voltage in terms of its ratio to coil terminal voltage. As can be seen from Section 3.2, there is a spread in inductance among windings in the coil. Thus, we treat every winding as a one-turn coil, and assume multiple *RL* circuits connected in series as shown in Figure 8. Let $R_{(s,n)}$ and $L_{(s,n)}$ denote, respectively, parasitic resistance and inductance of winding $w_{(\mathrm{Layer,Turn})}$. Then, coil terminal voltage can be expressed as shown below:

$$\begin{aligned} v_{\mathrm{L}}(t) = (&R_{(1,1)} + R_{(1,2)} + \cdots + R_{(1,N)} \\ &+ R_{(2,1)} + \cdots + R_{(2,2M)}) i_{\mathrm{L}}(t) \\ &+ (L_{(1,1)} + L_{(1,2)} + \cdots + L_{(1,N)} \\ &+ L_{(2,1)} + \cdots + L_{(2,N)}) \frac{di_{\mathrm{L}}(t)}{dt}. \end{aligned} \tag{7}$$

Here, we assume an inductive load; therefore, coil current $i_L \approx 0$ at maximum inductor voltage, and Equation (7) can be rewritten as shown below.

$$\begin{aligned} v_{\mathrm{L}}(t) = (&L_{(1,1)} + L_{(1,2)} + \cdots + L_{(1,N)} \\ &+ L_{(2,1)} + \cdots + L_{(2,N)}) \frac{di_{\mathrm{L}}(t)}{dt}. \end{aligned} \tag{8}$$

From Equation (8), it follows that voltage inside the coil is distributed by inductance of every winding. Equation (9) shows ratio of maximum interwinding voltage to coil terminal voltage. This parameter depending on the structure of improved solenoid coil can be used for evaluation of winding voltage.

$$\begin{aligned} \text{Ratio } A &= \frac{\text{Overall inductance at maximum winding voltage}}{\text{Total coil inductance}} \\ &= \frac{\sum_{s=1}^{2} \sum_{n=1}^{M} L_{(s,n)}}{L_{\mathrm{Coil}}}. \end{aligned} \tag{9}$$

Cross section of 14 to 6 turns coil is shown in Figure 9A; calculated induction for each winding of this coil is shown in Figure 9B. In the latter diagram, the horizontal axis plots winding inductance, and the vertical axis plots winding number. As can be seen from Figure 9, with 14 to 6 winding coil, difference in inductance between windings is about 1.5 times at maximum. Besides, the sum of inductances between $w_{(1,6)}$ and $w_{(2,6)}$ where the highest interwinding voltage occurs is 26.6 μH, while inductance of magnetic field generation coil

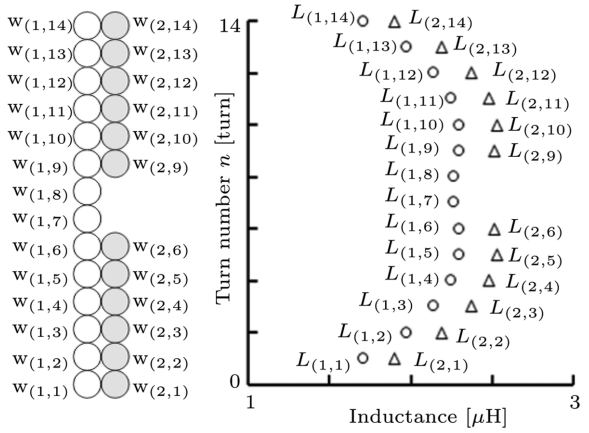

(a) Sectional view of 14-6 turns proposed coil structure

(b) Calculation result

FIGURE 9 Calculation results for inductance of each winding in 14 to 6 turns coil

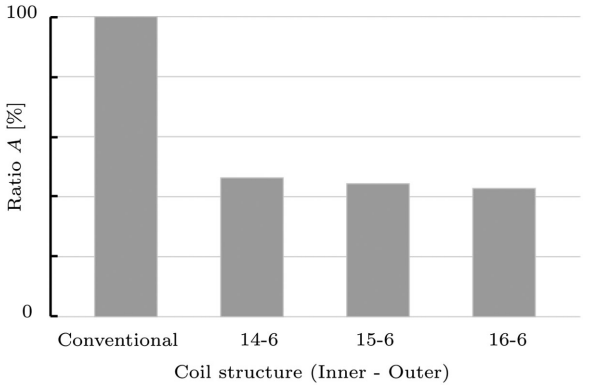

FIGURE 10 Calculation results for maximum voltage potential for each coil structure

is 57.8 μH; that is, maximum winding voltage can be reduced to 46.1% with respect to coil terminal voltage.

Ratio of maximum winding voltage to coil terminal voltage calculated by Equation (9) for conventional coil and improved solenoid coil with 14 to 6, 15 to 6, and 16 to 6 turns is shown in Figure 10. In the diagram, conventional coil and three structures meeting the constraints in Figures 6 and 7 are arranged on the horizontal axis, while ratio of maximum winding voltage to coil terminal voltage is plotted on the vertical axis. Figure 10 confirms that maximum winding voltage in the proposed structure can be greatly reduced as compared to conventional structure. For example, in case of 14 to 6 turns, the ration can be reduced to 46.1% against conventional solenoid coil. Analytic results in Figures 6 to 10 indicate that the proposed solenoid coil offers reduction of maximum voltage between windings, while providing same magnetic flux density as conventional coil.

TABLE 1 Comparison of three types of coil structure

Inner - Outer	16–6	15–6	14–6
Inductance	61.0 μH	59.4 μH	57.8 μH
Magnetic flux density	20.0 mT	20.1 mT	20.1 mT
Inductor voltage $V_{\mathrm{Lp-p}}$	9214 V	8972 V	8731 V
Ratio A	42.9%	44.4%	46.1%
Winding voltage $V_{\mathrm{maxp-p}}$	3953 V	3983 V	4025 V

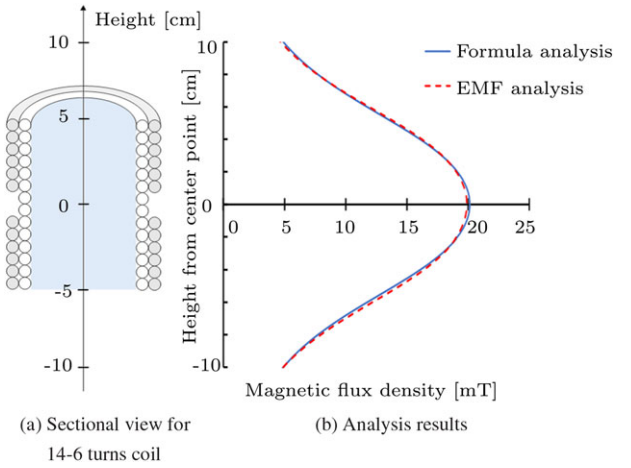

FIGURE 11 Comparison of magnetic flux density obtained by formula analysis and EMF analysis in 14 to 6 turns coil [Color figure can be viewed at wileyonlinelibrary.com]

3.5 | Consideration of improved solenoid coil

Table 1 compares analytic results obtained for three coil structures (14 to 6 to 16 to 6 turns) in case of sine current with frequency of 85 kHz and effective value of 100 A. As can be seen from the table, 14 to 6 turns coil offers the highest flux density; besides, coil terminal voltage is lower by about 500 V as compared to 16 to 6 coils, while winding voltage is nearly same. Thus, 14 to 6 turns coil is likely to be optimal structure for practical use, and we adopted this improved solenoid coil for magnetic field generation in this study.

3.6 | Verification of magnetic flux density through electromagnetic field analysis

We used electromagnetic field analysis to verify results for magnetic flux density obtained in Section 3.3. Particularly, we applied the finite integration technique (FIT) analysis using the electromagnetic simulation software CST EM STUDIO to 14 to 6 turns structure. Cross section of 14 to 6 turns coil is shown in Figure 11A. Here, coil center is defined as the origin. Results for magnetic flux density on the central axis calculated by Equation (6) and obtained by electromagnetic field analysis are presented in Figure 11B. In the diagram, the horizontal and vertical axes plot, respectively, flux density and height on coil's central axis, the origin being at coil center. Good agreement in flux density is obtained in Figure 11B, thus confirming adequacy of analytic formulas adopted in this study.

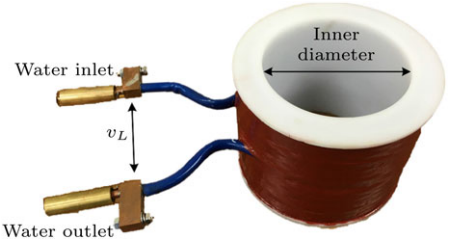

FIGURE 12 Coil for generating magnetic field [Color figure can be viewed at wileyonlinelibrary.com]

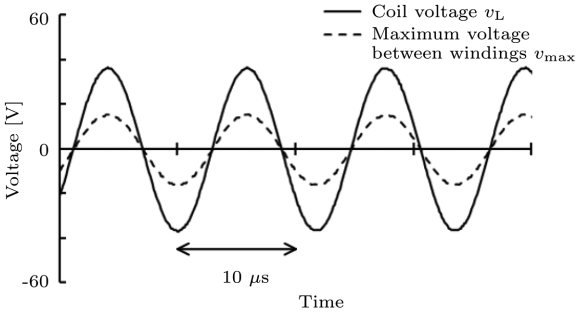

FIGURE 13 Measured results for winding voltage

4 | EXPERIMENTAL VERIFICATION USING PROPOSED COIL

4.1 | Experimental verification of winding voltage

We carried out experimental verification of winding voltage analysis for 14 to 6 turns coil in Section 3.4. The experimental coil for magnetic field generation is shown in Figure 12. In this experiment, 85-kHz sine current was passed through the experimental coil to measure coil terminal voltage and maximum interwinding voltage. Thus, obtained results are presented in Figure 13. Voltage between windings reaches 22.5 V at coil terminal voltage of 51.2 V, the ratio being 43.2%. This result is close to the theoretical value of 46.1%. Thus, we confirmed that voltage between windings can be reduced with the proposed coil structure, thus mitigating the risk of dielectric breakdown between the windings.

4.2 | Experimental verification of continuous operation

4.2.1 | Power supply

This verification experiment was conducted using the circuit in Figure 14. In this verification circuit, *LC* series resonant circuit is connected to the output of a single-phase full-bridge inverter. The inverter configured of 1200-V, 120-A

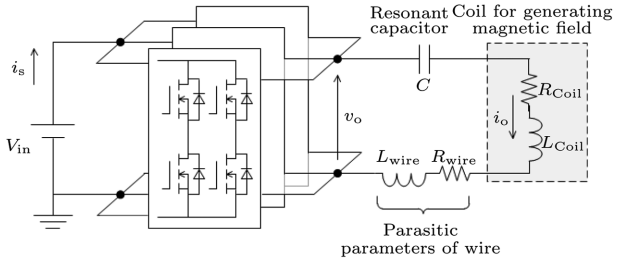

FIGURE 14 Circuit configuration

TABLE 2 Circuit conditions

Prameter	Value
Coil inductance L_{Coil}	58.5 μH
Coil resistance R_{Coil}	367 mΩ
Wire inductance L_{wire}	3.0 μH
Wire resistance R_{wire}	90 mΩ
Resonant capacitance C	70 nF
Resonant frequency f_r	76.7 kHz
Switching frequency f_s	82 kHz
Impedance Z	3.99 Ω

SiC-MOSFET (ROHM BSM120D12P2C005) outputted square wave voltage. Three inverter modules were connected in parallel to ensure output current. In this experimental setup, the magnetic field generation coil was placed at a distance of 1.5 m from the inverter so that magnetic flux generated by the coil does not affect other devices. For this reason, LC resonant circuit include parasitic components related to wiring. The experimental circuit parameters are given in Table 2. Inductances of the magnetic field generation coil and wiring are 58.5 μH and 3.0 μH, respectively. Resonant capacitor was configured as two series and two parallel connections of metallized polypropylene film capacitors (RUBYCON U102HVC703KLVR778, 70 nF). Rated voltage and current of the 70-nF resonant capacitor were set to 20 kV and 100 A, respectively. Thus, resonant frequency of the system was 76.7 kHz.

4.2.2 | Experimental results

In this circuit, switching frequency was set to 82 kHz, which is higher than resonant frequency of *LC* series resonant circuit, so that the resonant circuit works as an inductive load as seen from the voltage-fed inverter. In so doing, power factor angle of the resonant load is $\phi = 83.4$.

Waveforms of inverter output voltage and coil current are shown in Figure 15. Table 3 shows the experimental results. As can be seen from the diagram, sine-wave output current with effective value of 106.4 A and frequency of 82 kHz flows under input dc voltage of 380 V. Inverter's power capacity is 31.9 kVA.

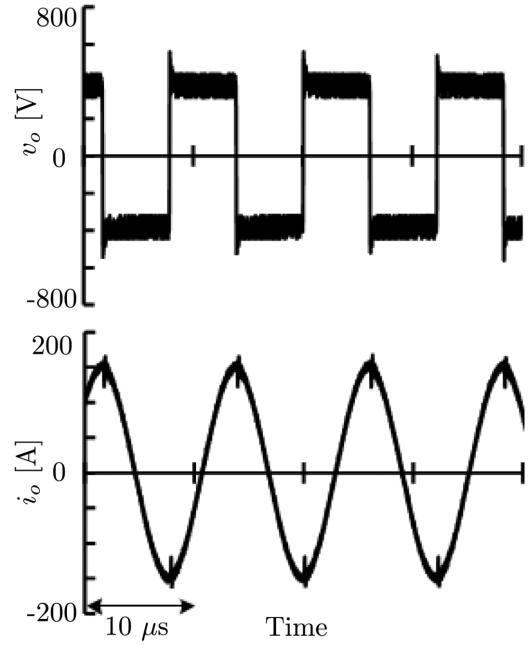

FIGURE 15 Experimental waveforms of output voltage and coil current with coil current set to 100 A

TABLE 3 Experimental results

Measured factor	Value
Input voltage V_{in}	380 V
Input current i_s	10.0 A
Output voltage v_o	380 V
Output current i_o	106.4 A
Inverter capacity	31.9 kVA

5 | CONCLUSION

In this study, we examined coil structure to generate 85-kHz magnetic field for evaluation of biological effects, and proposed an improved solenoid coil that meets constraints for both magnetic flux density and interwinding voltage. We demonstrated that with the proposed coil structure, maximum voltage between windings can be reduced less than half, while providing magnetic flux density same as in conventional solenoid coil. In addition, we designed and manufactured an experimental system consisting of a voltage-fed inverter and *LC* resonant circuit, and confirmed output current of 100 A, 82 kHz; thus, the proposed coil makes possible evaluation of biological effects.

ACKNOWLEDGMENT

This study was performed as a project sponsored by Ministry of Internal Affairs and Communications (Study on Non-thermal Biological Effects of Electromagnetic Fields in Intermediate Frequency Band (Particularly, Magnetic Fields in 100-kHz Band). Besides, we express our gratitude to Messrs.

Y. Ohnuma and S. Miyawaki from Nagaoka Power Electronics Co., Ltd. for their cooperation in inverter's design and fabrication.

REFERENCES

1. Shimode D, Murai T, Fujiwara S. A study of structure of inductive power transfer coil for railway vehicles. *IEEJ J Ind Appl*. 2015;4:550–558.
2. Shoji H, Uruno J, Isogai M, Yanagidaira T. Buck-boost-full-bridge inverter for all-metals induction heating cookers. *IEEJ J Ind Appl*. 2016;5:339–346.
3. Zingerli CM, Nussbaumer T, Kolar JW. Optimizing repulsive Lorentz forces for a levitating induction cooker. *IEEJ J Ind Appl*. 2015;4:439–444.
4. Imura T, Hori Y. Maximizing air gap and efficiency of magnetic resonant coupling for wireless power transfer using equivalent circuit and Neumann formula. *IEEE Trans Ind Electron*. 2011;58:4746–4752.
5. Li S, Mi C. Wireless power transfer for electric vehicle applications. *IEEE J Emerg Sel Topics Power Electron*. 2014;3:4–17.
6. Choi S, Huh J, Lee WY, Lee SW, Rim CT. New cross segmented power supply rails for roadway-powered electric vehicle. *IEEE Trans Power Electron*. 2013;28:5832–5841.
7. Kien Trung N, Ogata T, Tanaka S, Akatsu K. Analysis and PCB design of class D inverter for wireless power transfer systems operating at 13.56 MHz. *IEEJ J Ind Appl*. 2015;4:703–713.
8. Taki M. Bioelectromagnetics researches in Japan for human protection from electromagnetic field exposures. *IEEJ Trans Electr Electron Eng*. 2016;11:683–695.
9. Ushiyama A, Ohtani S, Suzuki Y, Wada K, Kunugita N, Ohkubo C. Effects of 21-kHz intermediate frequency magnetic fields on blood properties and immune systems of juvenile rats. *Int J Radiat Biol*. 2014;90:1211–1217.
10. Yoshie S, Ogasawara Y, Ikehata M, et al. Evaluation of biological effects of intermediate frequency magnetic field on differentiation of embryonic stem cell. *Toxicol Rep*. 2016;3:135–140.
11. Kogure S, Wada K, Suzuki Y. Development of a magnetic-field generator at 20 kHz using a voltage-source inverter for biological research. *European Conference on Power Electronics and Application*, 2009.
12. Wada K, Hayashi S, Suzuki Y. Design and implementation of multi-frequency magnetic field generator producing sinusoidal current waveform for biological researches. *European Conference on Power Electronics and Application*, 2016:8.
13. Wada K, Matsubara K, Yoshino H, et al. Development of an exposure system for 85 kHz magnetic field for the evaluation biological effects. *IEEE PELS Workshop on Emerging Technologies: Wireless Power Transfer (WoW)*, 2016:158–161.
14. Fujita A, Kawahara Y, Inoue S, Omori H. Development of a higher power intermediate-frequency magnetic field exposure system. *Bioelectromagnetics*. 2009;31:156–163.
15. Matsubara K, Wada K, Suzuki Y. Experimental evaluation of magnetic field generator for 100 kHz class. *Annual Meeting Record IEEJ*. 2016. (in Japanese)
16. Goto K, Yamazaki S. *Workbook on Electromagnetism*. Japan: Kyoritsu Shuppan; 2013. (in Japanese)

AUTHORS' BIOGRAPHIES

Kazuki Matsubara (student member) born in 1994. In 2016, he graduated from Tokyo Metropolitan University (Faculty of Pedagogy) where he started first term of doctorate (Graduate School of Science and Engineering, Electrical and Electronic Engineering). Matsubara's research interests include coil structure for magnetic field exposure systems.

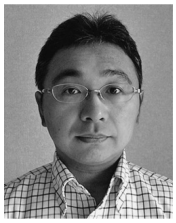

Keiji Wada (senior member) born in 1973. In 2000, he completed doctorate at Okayama University. Doctor of Eng. In 2000, he employed as an assistant by Tokyo Metropolitan University and Tokyo Institute of Technology (Graduate School of Science and Technology, Electrical and Electronic Engineering). Since 2006, he has been an adjunct professor at Tokyo Metropolitan University (Graduate School of Science and Engineering, Electrical and Electronic Engineering). Wada's research interests include power electronics.

Yukihisa Suzuki (member) born in 1970. In 1993, he graduated from Osaka University (School of Engineering, Nuclear Power Engineering), where he completed doctorate in 2001 (Graduate School of Engineering). Doctor of Eng. He is currently a professor at Tokyo Metropolitan University (Graduate School of Science and Engineering, Electrical and Electronic Engineering). Suzuki's research interests include bioelectromagnetics, numerical electromagnetic field analysis, plasma science, and engineering.

How to cite this article: Matsubara K, Wada K, Suzuki Y. Design of a coil geometry for generating magnetic field to evaluate biological effects at 85 kHz. *Electr Eng Jpn*. 2018;205:55–63. https://doi.org/10.1002/eej.23117

APPENDIX: REQUIRED OUTPUT MAGNETIC FLUX DENSITY

The target of output magnetic flux density in this study is based on ICNIRP Guidelines (revised edition of 2010). Experimental system for evaluation biological effects considered in this study is supposed to be subject to ICNIRP basic restrictions on electric field induced in human body (but not on

magnetic field [magnetic flux density] of biological origin). Besides, ICNIRP guidelines are configured of two stages—basic restrictions and reference levels; from the standpoint of human body protection, the point is whether basic restrictions are met or not. To protect human body from acute biological effects in 85-kHz band, basic restriction for internal electric field (occupational exposure) is set to $2.7 \times 10^{-4} f$ [V/m] (here f is frequency, and the restriction is 23 V/m). Thus, humans may be exposed to internal electric field limited by 23 V/m. Therefore, exposure to internal electric field for test animals at 85 kHz is set about the said value of 23 mV or its multiple. On the other hand, magnetic field generator considered in this study assumes experiments with mice. When exposed to uniform magnetic field of same strength, electric field induced in mice is much weaker than in humans. This follows intuitively from Faraday's law because magnetic flux is extremely low. Therefore, in computer simulations (dosimetry), exposure to uniform magnetic field about 10 mT is necessary to induce in a whole mouse body electric field with average strength of 23 V/m stipulated as the basic restriction. In order to produce internal electric field twice as strong as the basic restriction and to acquire response data in animal experiments, the evaluation system must ensure exposure to magnetic field of 20 mT or more.